Measuring Technetium-99m-MAG3 Clearance with an Improved Camera-Based Method

Andrew Taylor, Jr., Patti L. Corrigan, James Galt, Ernest V. Garcia, Russell Folks, Margie Jones, Amita Manatunga and Dennis Eshima

Division of Nuclear Medicine, Department of Radiology, and School of Public Health, Emory University School of Medicine, Atlanta, Georgia

Because commercially available camera-based methods are not optimized, they fail to account for dose infiltration, table attenuation and correspondence between time of injection and starting the camera. We have developed a more optimized technique to calculate camera-based clearances and applied this technique in the design of a camera-based clearance method for ^{99m}Tc-MAG3. **Methods:** Technetium-99m-MAG3 scintigraphy was performed in 20 patients who had varying degrees of renal function. Data were acquired posteriorly in supine patients at 2 sec/frame for 24 frames, 15 sec/frame for 16 frames and 30 sec/frame for 40 frames. Background correction was performed using an automated elliptical region of interest. Renal depth was estimated using improved regression equations and an empirically determined attenuation coefficient derived from phantom studies. Corrections were made for table attenuation and time discrepancies between dose injection and starting the camera. The percent injected dose in the kidney at 1–2, 1–2.5 and 2–3 min postinjection and the percent injected dose at those time periods corrected for body surface area were correlated with MAG3 clearance based on a single injection, two-compartment model. **Results:** There was high correlation between the percent injected dose in the kidney at all three time periods and the multisample clearance. Correcting for body surface areas significantly improved the correlation coefficients. Consequently, regression equations were developed to predict multisample clearance based on percent dose and body surface area. **Conclusion:** The optimization features described in this method should improve precision when sequential studies are conducted in the same patient.

Key Words: camera-based clearance; technetium-99m-MAG3 clearance

Technetium-99m-mercaptoacetyltriglycine (MAG3) is a renal imaging agent that is excreted from the body at essentially the same rate as ^{131}I-hippurate (OIH) (*1–4*). Because of the ^{99m}Tc label, MAG3 provides superior image quality than [^{131}I]OIH and substantially less radiation to the patient in individuals with impaired renal function (*5*). The clearance of MAG3 is proportional to the effective renal plasma flow (OIH clearance) and can be used as an index of renal function (*3,6–10*). The favorable dosimetry and superior clinical applications of ^{99m}Tc-MAG3 have resulted in increased clinical use since its introduction in 1992 so that it now accounts for approximately 40% of the estimated 420,000 renal scans performed annually in the United States.

Clearance measurements can serve as an important aid in the interpretation of renal scintigraphy. Techniques have already been developed and validated to measure the MAG3 clearance based on single- or dual-plasma samples (*11–13*), but plasma sample clearance methods require meticulous technique before reliable results can be obtained (*11,12*). With nuclear medicine evolving toward increased camera and computer sophistication, many technologists no longer have adequate in vitro experience to obtain reliable plasma sample measurements. Furthermore, the new regulations deriving from implementation of the Clinical Laboratory Improvement Act (CLIA) have added a new level of administrative requirements for laboratories handling blood and urine samples.

Camera-based clearance techniques are available commercially to measure the glomerular filtration rate (GFR) using ^{99m}Tc diethyltriaminepentaacetic acid (DTPA) and effective renal plasma flow (ERPF) using OIH (*14–17*); potential improvements have been suggested by several investigators (*18–20*). A preliminary camera-based technique to determine MAG3 clearance has been introduced and appears to give good results (*21,22*). This report, however, describes a camera-based technique to calculate MAG3 clearance which contains a number of optimized features, including an automated elliptical background region of interest (ROI), better estimation of renal depth, a more appropriate attenuation coefficient, correction for dose infiltration and table attenuation, correction for disparities between starting the camera and injecting the dose and an acquisition technique to correct for dose counting on cameras with different size fields of view.

TABLE 1
Results of Multisample MAG3 Clearance (Milliliter per Minute) and Body Surface Area (BSA)

Patient no.	Age	Sex	Height (cm)	Weight (kg)	MAG3 clearance	BSA
1	47	F	158.7	55.4	129	1.56
2	61	M	172.7	86	246	2.00
3	69	M	154	66	51	1.64
4	41	M	180.3	81	266	2.01
5	29	F	157.5	47.7	203	1.45
6	16	F	154.9	50	291	1.47
7	68	F	142.2	72	31	1.61
8	56	M	175.2	70	179	1.85
9	43	M	180.3	85	251	2.05
10	64	M	177.8	73.6	220	1.91
11	67	M	175.3	77.3	213	1.93
12	40	F	172.7	62.7	341	1.75
13	78	F	167.6	86.4	468	1.96
14	40	M	167.6	63.6	234	1.72
15	56	M	175.3	86.4	280	2.02
16	65	M	186.7	92.3	93	2.18
17	71	F	162.5	57.7	284	1.61
18	45	F	170.2	95.6	400	2.07
19	38	M	182.9	97.3	384	2.19
20	43	F	175	114	503	2.27

FIGURE 1. First 48 sec of data acquired at 2-sec intervals and displayed as a time-activity curve. The points representing 15% and 50% of the maximal activity were defined and extrapolated back to zero counts to define the time of the arrival of the bolus in each kidney. This time was defined as time zero.

MATERIALS AND METHODS

Patients

The study group initially consisted of 26 patients. Five patients were excluded because of dose infiltration exceeding 0.5%; a small amount of infiltration would not have much effect on the percent dose in the kidneys during the interval from 1 to 3 min postinjection, but it could potentially invalidate the multisample clearance that was used as the gold standard and requires a bolus injection. Another potential source of error is the gold standard itself, the multisample clearance. Dose infiltration, errors in preparing the standards or errors in drawing the blood samples can result in an incorrect clearance measurement. As a quality control procedure, we applied a modification of the Akaike Information Criterion, which provides an objective measure to evaluate the quality of the curve fit (23). Specifically, this criterion allows us to compare the actual plasma disappearance curve with the plasma disappearance curve predicted by the two-compartment model. One patient was excluded because of a poor fit (model selection criterion less than 3). The remaining 20 patients comprised the study population and are summarized in Table 1.

Data Acquisition and Time Zero

Data were acquired in a 128 × 128 matrix using a low-energy, all-purpose collimator. There was an initial 48-sec (twenty four 2-sec frames) acquisition followed by sixteen 15-sec frames and forty 30-sec frames for a total acquisition time of 24 min and 48 sec. To avoid timing errors due to injecting the dose prior to starting the camera or starting the camera before the dose was injected, time zero was defined as the time that the dose reached the kidney.

The time that the dose reached the kidney was determined by assigning a whole kidney ROI on the 2–3 min image and then generating a time-activity curve for each kidney during the first 48 sec after injection. The software automatically picks two points on the 48-sec time-activity curve which are 15% and 50% of the
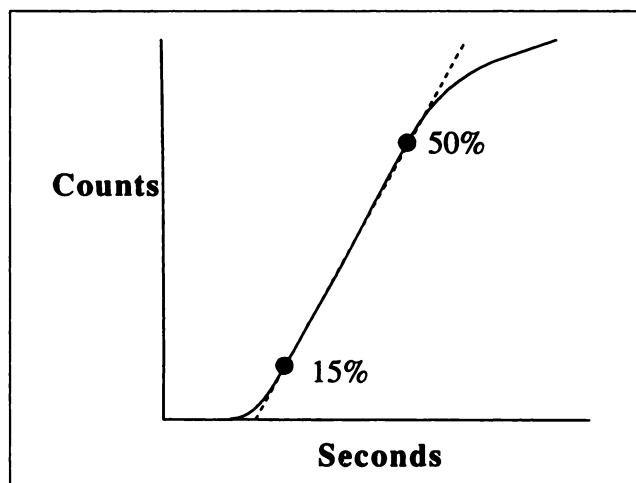
maximum value. By using these two points, the slope of the bolus curve is extrapolated back to zero counts to determine the time of bolus arrival in each kidney (Fig. 1). The time-activity curve and the linear extrapolation back to zero counts were displayed for each kidney and could be modified by the operator if the extrapolated line did not appear to fit the slope of the bolus. This could occur, for example, if the bolus were injected before starting the camera and the computer could not find 15% of the maximum activity. The initial 48-sec acquisition (2 sec/frame) was divided into three 16-sec intervals; time zero was defined as the beginning of the 16-sec interval in which the earlier of the two extrapolated renal curves intersected the x-axis.

Multisample Clearance

In each patient, MAG3 clearance was determined using the single-injection, two-compartment model of Sapirstein (24). This method has been described in detail and was based on a bolus injection followed by eight blood samples obtained from 5 to 60 min postinjection (11,12).

Background Correction

An automated elliptical ROI around each kidney was used to correct for background (25). The kidney ROIs were manually assigned. The elliptical background regions were generated by first drawing an imaginary box around the limits of the kidney ROI. The pixel coordinates were used to determine the width and height of the box. The background ROI was drawn as a double ellipse: each ellipse needs a major and minor axis. The major axis of the inner ellipse was the length of the box + 4 pixels; the minor axis was the width of the box + 4 pixels. For the outer ellipse, the major axis was the major axis of the inner ellipse + 3 pixels. The minor axis was the minor axis of the inner ellipse + 3 pixels. The area within the double ellipse defined the background ROI. The counts per pixel in the background ROI were normalized to the number of pixels in the kidney ROI and subtracted from counts in the kidney ROI to determine the background-corrected counts. The background-corrected counts were then corrected for renal depth and attenuation as described below.

Renal Depth

We used an improved formula to estimate renal depth that was derived from CT measurements in 200 supine patients: Left renal depth (mm) = 161.7 weight/height + 0.27 age − 9.4 and right renal depth (mm) = 151.3 weight/height + 0.22 age − 0.77, in which weight is in kilograms and height is in centimeters (26,27).

Table Attenuation

The table attenuation for two separate imaging tables was measured using a low-energy, all-purpose collimator and a 128 × 128 matrix resolution. With the gamma camera pointing up, a syringe containing approximately 350 μCi [^{99m}Tc] pertechnetate was placed on the collimator surface and counted for 1 min. The imaging table was then placed over the gamma camera so that the bottom of the table touched the collimator surface. The syringe was taped on the table surface at 2-cm increments across the width of the table and syringe counts were measured for 1-min intervals. These counts were decay-corrected and the table attenuation was obtained by averaging the percent table attenuation at these 16 points. Based on these data, the attenuation coefficients for the two tables were calculated to be 1.069 and 1.043, respectively.

Attenuation Coefficient

The attenuation correction appropriate for a kidney sized distribution of activity in tissue was determined from a phantom model. A 200-ml bottle (a 6.5 × 4.5-cm ovoid in a cross-section) filled with water was used to represent the kidney. The body was modeled with an elliptical SPECT phantom filled with water. Technetium-99m-pertechnetate (500 μCi) in approximately 1 ml were imaged for 120 sec. The activity was injected into the 200-ml bottle filled with water, which was placed in the elliptical phantom and imaged at depths (measured from the center of the bottle to the outside edge of the phantom) ranging from 3.5 to 13.5 cm. The same ROI was placed over each bottle image; counts were then extracted from each image and corrected for decay. The counts were plotted (counts versus depth) and fit with an exponential curve. The counts extracted from the original small volume were used as the intercept (no attenuation). The resulting attenuation correction was CF = exp (0.137/cm)(x − 1.1 cm), in which CF is the correction factor and x is the depth in centimeters. The factor of 1.1 cm can be attributed to the distribution of activity throughout a volume (the factor should be zero for a point source).

Dose Infiltration

At the completion of the study, an image was obtained over the injection site. If any infiltration was noted, a tight ROI was drawn around the area of infiltration and the counts were decay-corrected and divided by the counts injected. There was no correction for depth or attenuation. If infiltration exceeded 0.5%, the patient was excluded from the study.

Counting the Dose Injected

The syringe containing the dose was counted by placing it in a syringe holder parallel to the face of the camera; the syringe holder is 30 cm above the face of the camera. The postinjection syringe was also counted on the camera and residual activity was corrected for decay and subtracted from the preinjection syringe counts to yield the dose injected. Because the total counts depend on the area of the counting surface and because cameras may differ in crystal size, the technologist centered a square ROI (48 × 48 pixels, approximately 15 × 15 cm) over the dose and postinjection syringe to maintain a uniform area.

Deadtime losses are approximately 1% when 1.5 mCi were counted on the GE ACT camera (Milwaukee, WI). Most of the patients received 1.5 mCi or less. Larger administered doses were corrected for deadtime losses based on a calibration curve for the specific camera used in the study.

Percent Injected Dose in the Kidneys

The percent injected dose in the kidneys for various time periods in the interval between 1 and 3 min postinjection was determined using the following equation:

$$\frac{(TAF)(\text{left kidney counts} - \text{background})}{e^{-0.137(x - 1.1)}}$$
$$+ \frac{(TAF)(\text{right kidney counts} - \text{background})}{e^{-0.137(x - 1.1)}} \bigg/ \text{counts injected,}$$

where x is the renal depth, 0.137 is the effective attenuation coefficient of ^{99m}Tc in tissue and TAF is the table attenuation factor; counts injected were determined by counting the pre- and postinjection syringe over the camera (see below). Because of the framing rate, the interval we describe as 1–2 min, for example, was actually 63–123 sec.

Correction for Body Surface Area

The optimized software described above was used to calculate the percent injected dose in the kidneys at various time periods within the 1–3-min period postinjection for the 20 patients. The percent injected dose was also corrected for body surface area (BSA) that was calculated as follows:

$$BSA(m^2) = (W^{0.425})(H^{0.725})(71.84)/10,000,$$

where W is weight in kilograms and H is height in centimeters (28).

Statistical Analysis

To predict the multisample clearance based on the percent dose in the kidney at time points 1–2, 1–2.5 and 2–3 min, a series of regression equations were fitted. First, the regression line multisample clearance versus percent dose in the kidney was fitted for each time interval. Second, the variable BSA was added to the model to correct for BSA. For predictive purposes, a final model was developed with a single variable representing BSA and the percent dose in the kidney.

RESULTS

There was high correlation (r ≥ 0.9) between the percent injected dose in the kidney and the multisample clearance for all three time periods. The regression equation for percent dose in the kidney at 1–2.5 min was as follows: Technetium-99m-MAG3 clearance = 12.1 (% dose at =1–2.5 min) − 10.4, R^2 = 85%. After correcting for body surface area (see equation below), the total variation (R^2) explained by the regression line improved from 85% to 95%, which represented a significant improvement in the predictive power of the regression equation (p < 0.0001). Therefore, a better regression equation could be obtained after correcting for BSA. A single variable (BSA/1.73 × percent dose in the kidney) was used to develop the final regression equations that improved the correlation coefficients from ≥0.9 for the three equations to ≥0.96. The percent dose corrected for BSA at 1–2, 1–2.5 and 2–3 min were highly
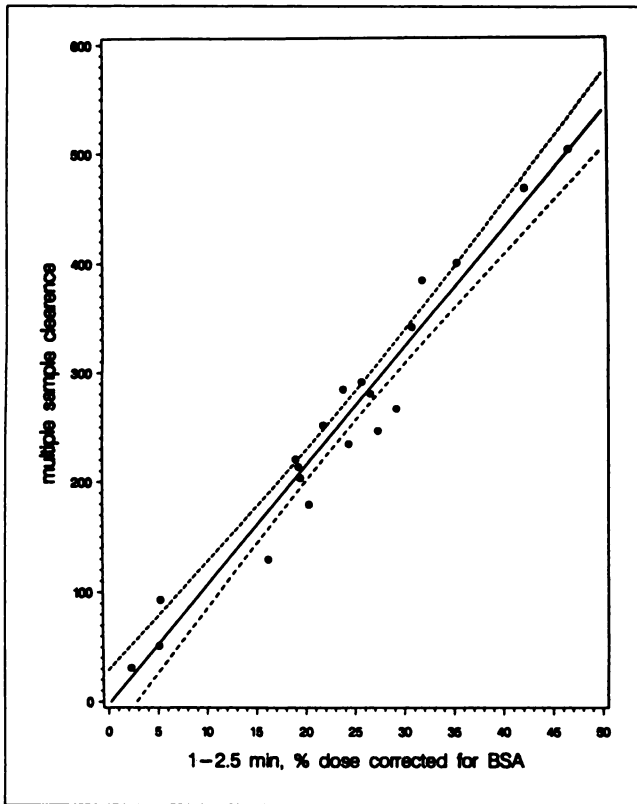
FIGURE 2. Regression line shows the relationship between the percent injected dose 1–2.5 min postinjection corrected for BSA and the multisample ^{99m}Tc-MAG3 clearance. The dotted lines show the 95% confidence limits.

correlated to each other with all correlations greater than 0.99. Therefore, the predictive power of all three regression equations was approximately the same.

The regression equations for the ^{99m}Tc-MAG3 clearance (CL) based on the percent dose in the kidney at 1–2, 1–2.5 and 2–3 min corrected for BSA are given below:

CL(1–2 min) = 17.6(% dose at 1–2 min)

$$(BSA/1.73 \text{ m}^2) + 2.5$$

CL(1–2.5 min) = 10.8(% dose at 1–2.5 min)

$$(BSA/1.73 \text{ m}^2) - 2.5$$

CL(2–3 min) = 13.2(% dose at 2–3 min)

$$(BSA/1.73 \text{ m}^2) - 4.7.$$

The standard error of the slope was 1.2, 0.6 and 0.7 for the equations at 1–2 min, 1–2.5 min and 2–3 min, respectively, the standard error of the intercept was 18.1, 14.9 and 15.4, respectively, and the variation (R^2) was 93%, 95% and 95%, respectively. The data comparing the percent dose in the kidney at 1–2.5 min postinjection corrected for BSA are shown in Figure 2. The dotted lines represent the 95% prediction interval around the regression line. This means that for the percent dose in the kidney corrected for

BSA in any given individual, we can be 95% confident that the true clearance value lies between the lower and upper limit of the confidence interval. For example, if the measured ^{99m}Tc-MAG3 clearance was 400 ml/min, we could use Figure 2 and be 95% certain that the true value lay approximately between 376 and 424 ml/min.

DISCUSSION

Dose infiltration exceeding 0.5% occurred in 5 of the first 21 patients. Most of these patients were injected by direct venipuncture. Subsequently, a catheter was inserted prior to injection and the dose was injected through the catheter. This procedure has minimized the problem of dose infiltration, which can invalidate the plasma sample or camera-based clearances; imaging over the injection site proved to be a valuable quality control procedure.

The Tonnesen equations for renal depth used in the Schlegel and Gates camera-based method were derived from an ultrasonic measurement of renal depth with the patient in a sitting position and the probe angled obliquely to the kidney (14–17,29). Since most renal studies are performed with the patient supine and the camera placed beneath the patient, the Tonnesen equations do not provide an optimal estimate for renal depth and the error increases as the depth increases (26). In these studies, we have used improved renal depth correction equations based on CT measurements in 200 supine patients. The new depth equations provide a much better estimate of renal depth than the Tonnesen equations (26,27).

Correction for table attenuation minimizes another potential source of error. In our institution, there was a 2.6% difference in attenuation correction for the tables used in renal studies. This difference is small and would only result in an error of 5 ml/min in a patient with a ^{99m}Tc-MAG3 clearance of 200 ml/min if we used the same attenuation for both tables. There may be, however, greater differences in tables from different manufacturers and the addition of correction for table attenuation may provide better comparison data for camera-based clearances, especially when measurements are performed on tables provided by different suppliers.

The linear attenuation coefficient for ^{99m}Tc in tissue is 0.153/cm and this value is used in most commercial GFR protocols; however, the effective attenuation is actually due less to scatter. We measured effective attenuation using a renal phantom in a water bath and used our measurements of effective attenuation to correct for renal depth. Our value of 0.137/cm was similar to those reported by Fleming (0.12/cm), Cosgriff (0.11/cm) and Corrigan (0.14/cm) (30–32). A simple linear attenuation factor assumes a point source; however, the kidney is a distributed source and a distributed source is not equivalent to a point source at the center of the volume. The size and shape of the volume have an effect on the measured counts primarily because of self-attenuation and Compton scatter. To determine the true counts, we initially counted the dose in a

small volume of approximately 1 ml before placing it in the 200-ml phantom. The empirically determined 1.1-cm value in our attenuation correction factor, exp (0.137/cm)(x − 1.1 cm), helps compensate for the kidney as a distributed source. More accurate attenuation correction should improve the accuracy of measuring accumulation ^{99m}Tc-MAG3 or any ^{99m}Tc radiopharmaceutical in the kidney.

Counts in the renal ROI in the 1–3-min postinjection period are a function of actual tracer clearance by the kidney plus background activity due to tracer present in the tissue anterior and posterior to the kidney, blood-pool activity within the kidney and activity in the interstitial space of the kidney. An accurate measurement of renal clearance requires a precise background correction. In this respect, MAG3 has an inherent advantage over DTPA because it is extracted much more efficiently by the kidney. In normal volunteers, for example, the 2–3-min renal uptake of MAG3 was almost twice as great as the 2–3 min renal uptake of DTPA (5). Consequently, the kidney-to-background ratio is higher for MAG3 than DTPA and errors due to background selection will not have as great an effect.

Regardless of the radiopharmaceutical used, however, background correction is problematic and is accentuated in patients with poor renal function because of the reduced kidney-to-background ratio. Furthermore, variations in background ROIs can affect measurements of absolute and relative renal function, especially in patients with impaired function. Different individuals may assign backgrounds differently and even the same individual may assign different backgrounds at various times. To minimize interobserver and intraobserver variability, to better account for scatter from the liver into the kidney ROI and to obtain better reliability in sequential studies, we used an automated elliptical background ROI around each kidney. Elliptical or perirenal background subtraction appears to be the procedure of choice for ^{99m}Tc-MAG3 studies (25).

We counted the dose by placing it in the syringe holder parallel to the face of the camera. If the dose exceeds a count threshold for a particular camera, deadtime losses will result, the injected dose will be underestimated and the clearance overestimated. If the injected dose does exceed the counting threshold of the camera, a correction for deadtime can be made using a calibration curve. Alternatively, a small dose can be counted that does not exceed the count capacity of the camera; the small dose and the dose to be injected can be counted in the dose calibrator and the ratio of the two can be used to determine the counts injected. The postinjection syringe should also be counted on the camera to correct for incomplete dose administration.

The mean kidney counts normalized to 1 mCi were displayed in 15-sec intervals from 1–3.5 min (Fig. 3). Based on these data, errors in sequential studies due to the 15-sec framing interval would be minimized by integrating over 2–3 min and the 2–3-min interval might be preferred for the regression equation. A potential limitation of the 2–3-min
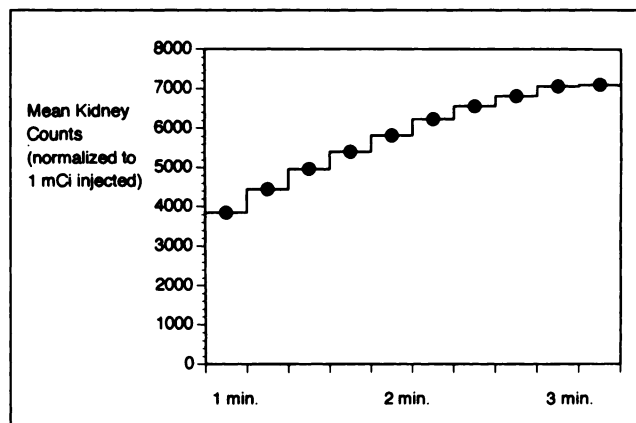

FIGURE 3. Pooled data for the 20 patients with mean counts in the kidney normalized to 1 mCi at 15-sec intervals from 1 to 3.5 min.

interval is the possibility that some of the tracer might be excreted from one or both kidneys during the 2–3-min period. This did not appear to be a problem in our patient population since the 1–2-, 1–2.5- and 2–3-min regression equations were all highly correlated and all fit the data equally well; however, rapid excretion could be a problem in an individual patient.

To minimize processing time, we used a three-phase acquisition. Time zero was defined as the beginning of the 16-sec interval in which the earlier of the two extrapolated renal curves intersected the x-axis. This framing rate limits the error in defining time zero to 16 sec; in sequential studies, for example, if the bolus intersected the x-axis at 16 sec, time zero would be defined as 0 sec; if the bolus intersected the x-axis at 17 sec, time zero would be defined as 17 sec. With improved hardware, a more rapid framing rate and integration at 1–2 or 1–2.5 min would be preferable.

One problem with basing clearance on the percent uptake in the kidney is that the uptake is partially dependent on blood volume (33). An empirical clearance estimation based on the early uptake of a tracer assumes instantaneous mixing and that the quantity of tracer transferred from the extracellular space back into the plasma is negligible. According to these assumptions, the percentage uptake during the 1–3 min postinjection period should be approximately proportional to the clearance expressed as a percent of the plasma volume (30). Since plasma volume is proportional to body size, the correlation might be improved by correcting the clearance for body size. This concept is somewhat analogous to using a standardized uptake value (SUV) for [^{18}F] fluorodeoxyglucose or other diffusible tracers. For example, Kim et al. (34) have pointed out that the measurement of relative uptake value of most diffusible tracers may be improved with a correction for BSA and Mulligan et al. (35) have reported that the Gates equation correlated better with the GFR when corrected for BSA. Consequently, we derived one regression equation to convert the percent dose of MAG3 in the kidneys to MAG3 clearance and a second regression equa-

tion that corrected the percent dose in the kidney for BSA and then converted this BSA corrected value to MAG3 clearance. In our patient population, there was significant improvements in the results when we corrected for BSA.

Serum creatinine is the most common measure of renal function in current clinical practice, but it is not an accurate index of GFR; at best, it is a rough guide (36). A patient may lose up to 50% of renal function before the serum level of creatinine increases to an abnormal value. There is a wide range of values for serum creatinine at all levels of inulin clearance (GFR), and creatinine can remain within the normal range despite inulin clearances up to 60% below normal (36). A formal measurement of creatinine clearance with blood and 24-hr urine samples is cumbersome and may be an unreliable method of evaluating renal function (37).

Camera-based clearances appear to provide a more reliable measure of renal function than serum creatinine or creatinine clearance (38). Although they are not as accurate as plasma sample clearances, camera-based clearances are highly reproducible in stable patients. Gates reported a correlation coefficient of 0.99 between camera-based GFR measurements repeated on different days in stable patients (16). Chachati et al. also compared the reproducibility of the Gates and Schlegel techniques in 10 stable patients (20 kidneys) 7 days apart and also found excellent reproducibility, r = 0.91 for GFR and 0.95 for ERPF (39). Finally, Klingensmith et al. (40) recently compared the renal uptake of ^{99m}Tc-MAG3 at 1–2 min as a percent of the injected dose in 36 patients studied at least 2 days apart and reported excellent reproducibility (r = 0.99).

CONCLUSION

MAG3 is widely used and is considered to be superior to DTPA by the United Kingdom Renography Standardization Group (41). A camera-based clearance technique for ^{99m}Tc-MAG3 has been developed with optimized features that are easily incorporated by other centers. Its accuracy certainly appears to be comparable to that reported for camera-based clearance techniques using OIH and DTPA and the optimization procedures should improve the precision of the measurements (14–17,34,37–40,42–44). Given the errors associated with estimating renal depth from a regression equation (26), the results are actually better than we expected. Our camera-based method to determine ^{99m}Tc-MAG3 clearance will need testing in a larger population to better define its accuracy and limitations.

ACKNOWLEDGMENTS

REFERENCES

1. Taylor A, Eshima D, Christian PE, et al. A technetium-99m-MAG3 kit formulation: preliminary results in normal volunteers and patients with renal failure. *J Nucl Med* 1988;29:616–622.
2. Taylor AT, Eshima D, Fritzberg AR, et al. Comparison of iodine-131-OIH and technetium-99m-MAG3 renal imaging in volunteers. *J Nucl Med* 1988;27:795–803.
3. Taylor A, Ziffer JA, Steves A, et al. Clinical comparison of I-131-OIH and the kit formulation of Tc-99m mercaptoacectyltriglycine. *Radiology* 1986;170:721–725.
4. Eshima D, Taylor A. Technetium-99m mercaptoacetyltriglycine: update on the new Tc-99m renal tubular function agent. *Semin Nucl Med* 1992;22:61–73.
5. Stabin M, Taylor A, Eshima D, Wooten W. Radiation dosimetry for technetium-99m-MAG3, technetium-99m-DTPA and iodine-131-OIH based on human biodistribution studies. *J Nucl Med* 1992;33:33–40.
6. Russell CD, Thorstad B, Yester MV, et al. Comparison of technetium-99m-MAG3 with iodine-131-hippuran by a simultaneous dual-channel technique. *J Nucl Med* 1988;29:1189–1193.
7. Itoh K, Tsukamoto E, Kakizaki H, et al. Phase II study of Tc-99m MAG3 in patients with nephrourologic diseases. *Clin Nucl Med* 1993;18:387–393.
8. Jafri RA, Britton KE, Nimmon CC, et al. Technetium-99m-MAG3, a comparison with iodine-131-hippuran by simultaneous dual-channel technique. *J Nucl Med* 1988;29:147–148.
9. Bubeck B, Brandau W, Weber E, et al. Pharmacokinetics of technetium-99m-MAG3 in humans. *J Nucl Med* 1990;31:1285–1293.
10. Müller-Suur R, Bois-Svensson I, Meskol L. A comparative study of renal scintigraphy and clearance with technetium-99m-MAG3 and iodine-123-hippurate in patients with renal disorders. *J Nucl Med* 1990;31:1811–1817.
11. Russell CD, Taylor A, Eshima D. Estimation of technetium-99m-MAG3 plasma clearance in adults from one or two blood samples. *J Nucl Med* 1989;30:1955–1959.
12. Taylor A Jr, Corrigan P, Eshima D, Folks R. Prospective validation of a single sample technique to determine Tc-99m-MAG3 clearance. *J Nucl Med* 1992;33:1620–1622.
13. Bubeck B, Piepenburg R, Grethe U, Ehrig B, Hahn K. A new principle to normalize plasma concentrations allowing single-sample clearance determinations in both children and adults. *Eur J Nucl Med* 1992;19:511–516.
14. Schlegel JU, Halikiopoulos HL, Prima R. Determination of the filtration fraction using the gamma camera. *J Urol* 1979;122:447–450.
15. Schlegel JU, Hamway SA. Individual renal plasma flow determination in 2 minutes. *J Urol* 1976;116:2882–2285.
16. Gates GF. Glomerular filtration rate: estimation from fractional renal accumulation of Tc-99m DTPA (stannous). *AJR* 1982;138:565–570.
17. Gates GF. Split renal function testing using Tc-99m DTPA: rapid technique for determining differential glomerular filtration. *Clin Nucl Med* 1983;8:400–407.
18. Awdeh M, Kouris K, Hassan IM, Abdel-Dayem HM. Factors affecting the Gates' GFR measurement [Abstract]. *J Nucl Med* 1989;30(suppl):843.
19. Hurwitz GA, Champagne C, Gravelle DR, Smith FJ, Powe JE. The variability of processing of technetium-99m DTPA renography: role of interpolative background subtraction. *Clin Nucl Med* 1993;18:273–277.
20. Taylor A, Garcia E, Jones M, et al. An optimized camera-based technique to calculate Tc-99m-MAG3 clearance [Abstract]. *J Nucl Med* 1992;33(suppl):948.
21. Taylor A, Halkar RK, Garcia E, et al. A camera-based method to calculate Tc-99m-MAG3 clearance [Abstract]. *J Nucl Med* 1991;32(suppl):953.
22. Arroyo AJ. Effective renal plasma flow determination using technetium-99m-MAG3: Comparison of two camera techniques with the Tauxe method. *J Nucl Med Technol* 1993;21:162–166.
23. Akaike H. An information criterion (AIC). *Math Sci* 1976;14:5–9.
24. Sapirstein LA, Vidt DG, Mandel MK, et al. Volumes of distribution and clearances of intravenously injected creatinine in the dog. *Am J Physiol* 1955;181:330–336.
25. Thakore K, Folks R, Taylor A. The effect of different ROIs for background correction on relative renal function in patients with unilateral nephrectomy [Abstract]. *J Nucl Med* 1993;34(suppl):87P.
26. Taylor A, Lewis C, Giacometti A, et al. Improved formulas for the estimation of renal depth in adults. *J Nucl Med* 1993;34:1766–1769.
27. Taylor A. Formulas to estimate renal depth in adults [Letter]. *J Nucl Med* 1994;35:2054–2055.
28. Dubois D, Dubois EF. A formula to estimate the approximate surface area if height and weight be known. *Arch Intern Med* 1916;17:863–871.
29. Tonnesen KH, Munck O, Hald T, et al. Influence on the radiorenogram of variation in skin to kidney distance and the clinical importance hereof. In:

Zum Winkel K, Blaufox MD, Funck-Bretano JL, eds. *Proceedings of the International Symposium on Radionuclides in Nephrology*. Stuttgart: Thieme; 1974:79–86.

30. Fleming JS, Keast CM, Waller DG, Ackery D. Measurement of glomerular filtration with Tc-99m DTPA: a comparison of gamma camera methods. *Eur J Nucl Med* 1987;13:250–253.

31. Cosgriff P, Brown H. Influence of kidney depth on the renographic estimation of relative renal function [Letter]. *J Nucl Med* 1990;31:1576–1577.

32. Corrigan DM, Collis SA. Estimation of glomerular filtration rate, without blood sampling, during renography. *Clin Phys Physiol Meas* 1984;5:279–284.

33. Fawdry RM, Gruenewald SM, Collins LT, Roberts AJ. Comparative assessment of techniques for estimation of glomerular filtration rate with ^{99m}Tc-DTPA. *Eur J Nucl Med* 1985;11:7–12.

34. Kim CK, Gupta NC, Chandramouli B, Alavi A. Standardized uptake values of FDG: body surface area correction is preferable to body weight correlation. *J Nucl Med* 1994;35:164–167.

35. Mulligan JS, Blue PW, Hasbargen JA. Methods for measuring GFR with technetium-99m-DTPA: an analysis of several common methods. *J Nucl Med* 1990;31:1211–1219.

36. Levey AS, Madaio MP, Perrone RD. The kidney. In: Brenna BM, Rector FC, eds. *Laboratory assessment of renal disease: clearance, urinalysis and renal biopsy*. Philadelphia: W.B. Saunders; 1991:919–937.

37. Rosenbaum JL. Evaluation of clearance studies in chronic kidney disease. *J Chron Dis* 1970;22:507–514.

38. Russell CD, Dubovsky EV. Gates method for GFR measurement [Letter]. *J Nucl Med* 1986;27:1373–1374.

39. Chachati A, Meyers A, Godon JP, Rigo P. Rapid method for the measurement of differential renal function: validation. *J Nucl Med* 1987;28:829–836.

40. Klingensmith WC, Briggs DE, Smith WI. Technetium-99m-MAG3 renal studies: normal range and reproducibility of physiologic parameters as a function of age and sex. *J Nucl Med* 1994;35:1612–1617.

41. Cosgriff PS, Lawson RS, Nimmon CC. Towards standardization in gamma camera renography. *Nucl Med Commun* 1992;13:580–585.

42. Goates JJ, Morton KA, Wooten WW, et al. Comparison of methods for calculating glomerular filtration rate: technetium-99m-DTPA scintigraphic analysis, protein-free and whole-plasma clearance of technetium-99m-DTPA and iodine-125-iothalamate clearance. *J Nucl Med* 1990;31:424–429.

43. Ginjaume M, Casey M, Barker F, Duffy G. Measurement of glomerular filtration rate using technetium-99m-DTPA. *J Nucl Med* 1985;26:1347–1348.

44. Fine EJ, Axelrod M, Gorkin J, Saleemi K, Blaufox MD. Measurement of effective renal plasma flow: a comparison of methods. *J Nucl Med* 1987;28:1393–1400.